Uncertainty quantification in imaging and automatic horizon tracking—a Bayesian deep-prior based approach

Ali Siahkoohi, Gabrio Rizzuti, and Felix J. Herrmann

School of Computational Science and Engineering
Georgia Institute of Technology

Seismic imaging

estimate reflectivity $\delta\mathbf{m}$ given observed data $\{\mathbf{d}_i\}_{i=1}^{n_s}$

$$\min_{\delta \mathbf{m}} \quad \frac{1}{2\sigma^2} \sum_{i=1}^{n_s} \|\delta \mathbf{d}_i - \mathbf{J}(\mathbf{m}_0, \mathbf{q}_i)\delta \mathbf{m}\|_2^2$$

linearized Born operator, $\mathbf{J}(\mathbf{m}_0, \mathbf{q}_i)$

linearized data, $\delta \mathbf{d}_i$

noise variance, σ^2

Challenges

expensive forward operator

inconsistent, mildly ill-conditioned

2D slice from Parihaka dataset

finite-difference simulations w/ `Devito`

WesternGeco. *Parihaka 3D PSTM Final Processing Report*. Tech. rep. New Zealand Petroleum Report 4582. New Zealand Petroleum & Minerals, Wellington, 2012. URL: https://wiki.seg.org/wiki/Parihaka-3D.

M. Louboutin et al. "Devito (v3.1.0): an embedded domain-specific language for finite differences and geophysical exploration". In: *Geoscientific Model Development* 12.3 (2019), pp. 1165–1187. DOI: 10.5194/gmd-12-1165-2019. URL: https://www.geosci-model-dev.net/12/1165/2019/.

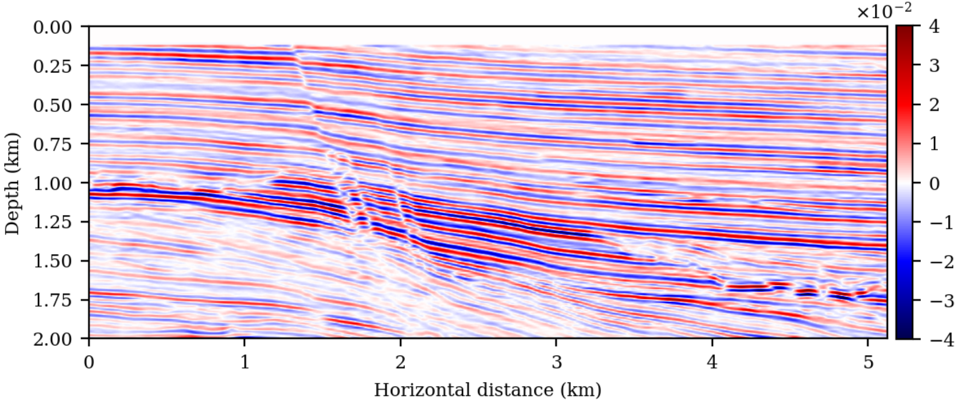

$\delta\mathbf{m}$—"true" reflectivity model obtain from Parihaka dataset

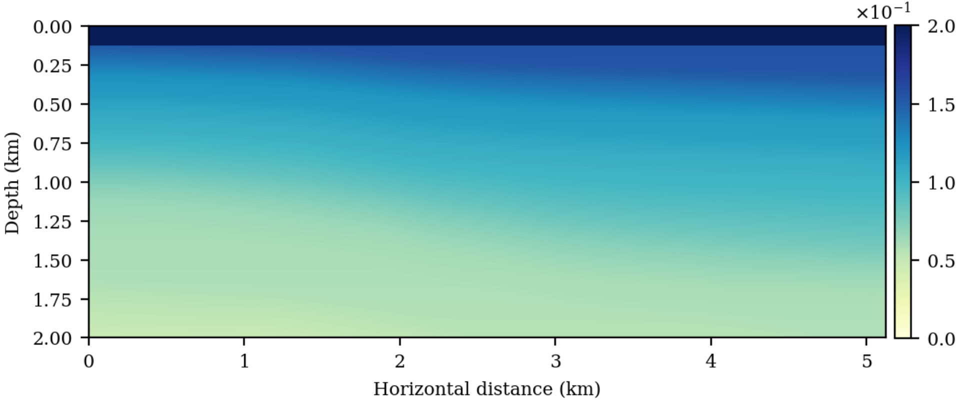

$\mathbf{m}_0$—made up background squared-slowness model $\left(\frac{\mathrm{s}^2}{\mathrm{km}^2}\right)$

205 sources w/ $25 \mathrm{~m}$ sampling rate

410 receivers w/ $12.5 \mathrm{~m}$ sampling rate

$1.5 \mathrm{~s}$ recording time

Ricker source wavelet w/ $30 \mathrm{~Hz}$ central frequency

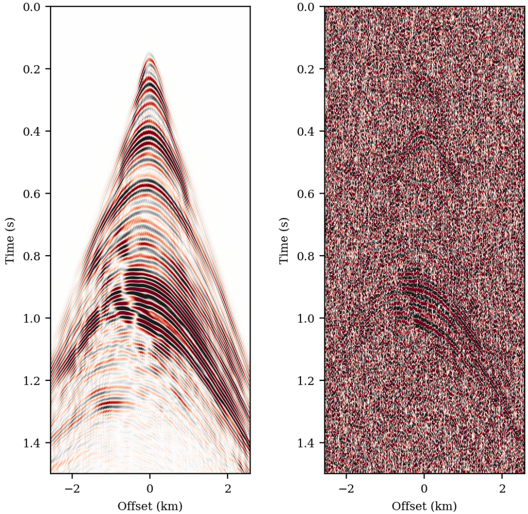

Noise-free (left) and noisy (right) linearized data — SNR: -8.7466 dB

Maximum likelihood estimate

$$\min_{\delta \mathbf{m}} \quad \frac{1}{2\sigma^2} \sum_{i=1}^{n_s} \|\delta \mathbf{d}_i - \mathbf{J}(\mathbf{m}_0, \mathbf{q}_i)\delta \mathbf{m}\|_2^2$$

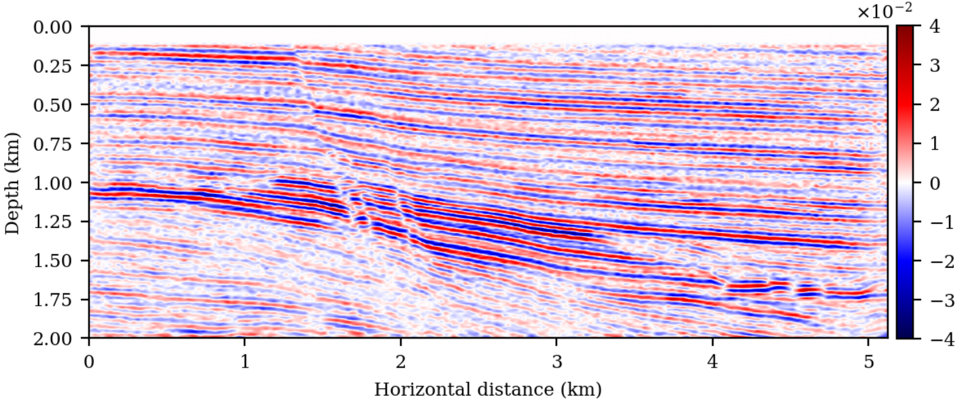

MLE—no regularization (prior)

Deep priors

regularization w/ an untrained CNN

V. Lempitsky, A. Vedaldi, and D. Ulyanov. "Deep Image Prior". In: *2018 IEEE/CVF Conference on Computer Vision and Pattern Recognition*. June 2018, pp. 9446–9454. DOI: 10.1109/CVPR.2018.00984.

Deep priors in seismic

data reconstruction

denoising

Qun Liu, Lihua Fu, and Meng Zhang. "Deep-seismic-prior-based reconstruction of seismic data using convolutional neural networks". In: *arXiv preprint arXiv:1911.08784* (2019).

Yunzhi Shi, Xinming Wu, and Sergey Fomel. "Deep learning parameterization for geophysical inverse problems". In: *SEG 2019 Workshop: Mathematical Geophysics: Traditional vs Learning, Beijing, China, 5-7 November 2019*. Society of Exploration Geophysicists. 2020, pp. 36–40. DOI: 10.1190/iwmg2019_09.1.

Deep priors in seismic

imaging

full-waveform inversion

Ali Siahkoohi, Gabrio Rizzuti, and Felix J. Herrmann. "A Deep-Learning Based Bayesian Approach to Seismic Imaging and Uncertainty Quantification". In: 2020.1 (2020), pp. 1–5. DOI: https://doi.org/10.3997/2214-4609.202010770. URL: https://arxiv.org/pdf/2001.04567.pdf.

Yulang Wu and George A McMechan. "Parametric convolutional neural network-domain full-waveform inversion". In: *GEOPHYSICS* 84.6 (2019), R881–R896. DOI: 10.1190/geo2018-0224.1.

Deep prior

$$\delta\mathbf{m} = g(\mathbf{z}, \mathbf{w}), \quad \mathbf{w} \sim \mathrm{N}(\mathbf{0}, \lambda^{-2}\mathbf{I})$$

untrained CNN, $g(\mathbf{z}, \mathbf{w})$

CNN weights, $\mathbf{w}$

fixed input, $\mathbf{z}$

V. Lempitsky, A. Vedaldi, and D. Ulyanov. "Deep Image Prior". In: *2018 IEEE/CVF Conference on Computer Vision and Pattern Recognition*. June 2018, pp. 9446–9454. DOI: 10.1109/CVPR.2018.00984.

Negative-log posterior

$$
\begin{aligned}
&- \log \pi_{\mathbf{w}|\delta\mathbf{d}} \left(\mathbf{w} \mid \{\delta\mathbf{d}_i\}_{i=1}^{n_s} \right) \\
&= \underbrace{\frac{1}{2\sigma^2} \sum_{i=1}^{n_s} \left\| \delta\mathbf{d}_i - \mathbf{J}(\mathbf{m}_0, \mathbf{q}_i) g(\mathbf{z}, \mathbf{w}) \right\|_2^2}_{\text{negative-log likelihood}} + \underbrace{\frac{\lambda^2}{2} \|\mathbf{w}\|_2^2}_{\text{negative-log prior}} + \underbrace{\text{const}}_{\text{Ind. of } \mathbf{w}}
\end{aligned}
$$

Posterior distribution, $\pi_{\mathbf{w}|\delta\mathbf{d}}$

MAP, conditional mean, pointwise standard deviation (UQ), ...

MAP estimate, $\widehat{\delta \mathbf{m}}_{\mathsf{MAP}} = g(\mathbf{z}, \widehat{\mathbf{w}}_{\mathsf{MAP}})$

$$\widehat{\mathbf{w}}_{\mathsf{MAP}} := \underset{\mathbf{w}}{\arg\max} \ \pi_{\mathbf{w} | \delta \mathbf{d}} \left(\mathbf{w} \mid \{ \delta \mathbf{d}_i \}_{i=1}^{n_s} \right)$$

conditional (posterior) mean, $\widehat{\delta\mathbf{m}}_{\text{CM}}$

$$\widehat{\delta\mathbf{m}}_{\text{CM}} := \mathbb{E}_{\mathbf{w}\sim\pi_{\mathbf{w}|\delta\mathbf{d}}}\left[g(\mathbf{z}, \mathbf{w})\right] \approx \frac{1}{n_{\text{w}}}\sum_{j=1}^{n_{\text{w}}} g(\mathbf{z}, \widehat{\mathbf{w}}_j),$$

samples from posterior, $\left\{\widehat{\mathbf{w}}_j\right\}_{j=1}^{n_{\text{w}}} \sim \pi_{\mathbf{w}|\delta\mathbf{d}}\left(\mathbf{w} \mid \left\{\delta\mathbf{d}_i\right\}_{i=1}^{n_s}\right)$

pointwise standard deviation (UQ)

$$\widehat{\boldsymbol{\sigma}}^2 := \frac{1}{n_{\mathrm{w}} - 1} \sum_{j=1}^{n_{\mathrm{w}}} \left(g(\mathbf{z}, \widehat{\mathbf{w}}_j) - \widehat{\delta \mathbf{m}}_{\mathsf{CM}} \right) \odot \left(g(\mathbf{z}, \widehat{\mathbf{w}}_j) - \widehat{\delta \mathbf{m}}_{\mathsf{CM}} \right),$$

samples from posterior, $\left\{ \widehat{\mathbf{w}}_j \right\}_{j=1}^{n_{\mathrm{w}}} \sim \pi_{\mathbf{w} \mid \delta \mathbf{d}} \left(\mathbf{w} \mid \{\delta \mathbf{d}_i\}_{i=1}^{n_s} \right)$

Comparison

MLE (no deep prior), MAP, and conditional mean

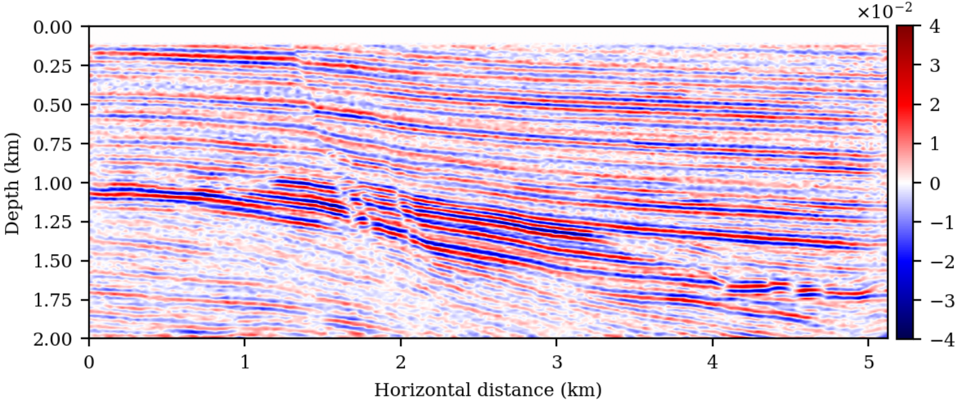

MLE—no (deep) prior

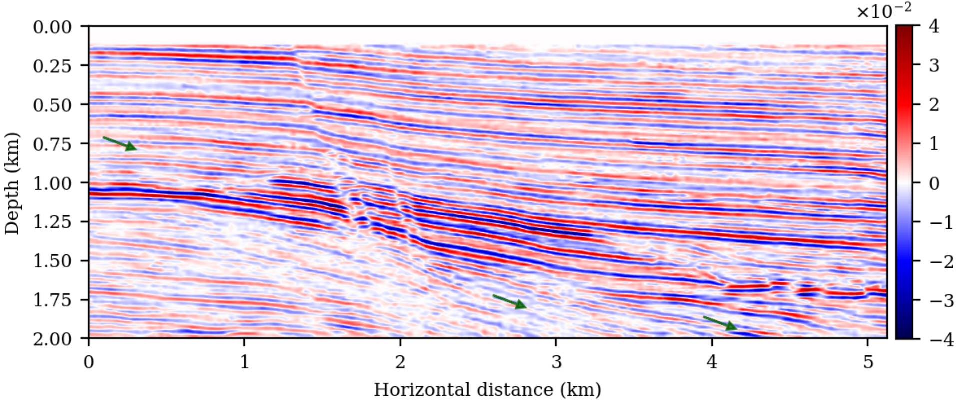

MAP estimate—SNR: 8.77 dB

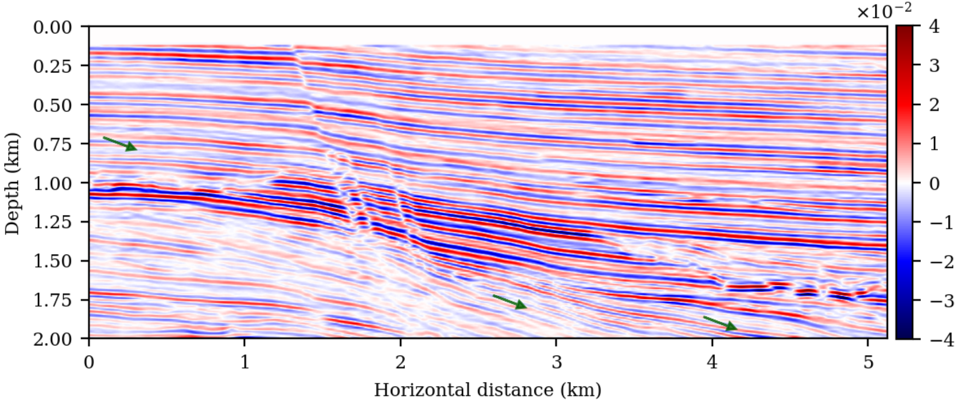

$\delta\mathbf{m}$—"true" reflectivity model obtain from Parihaka dataset

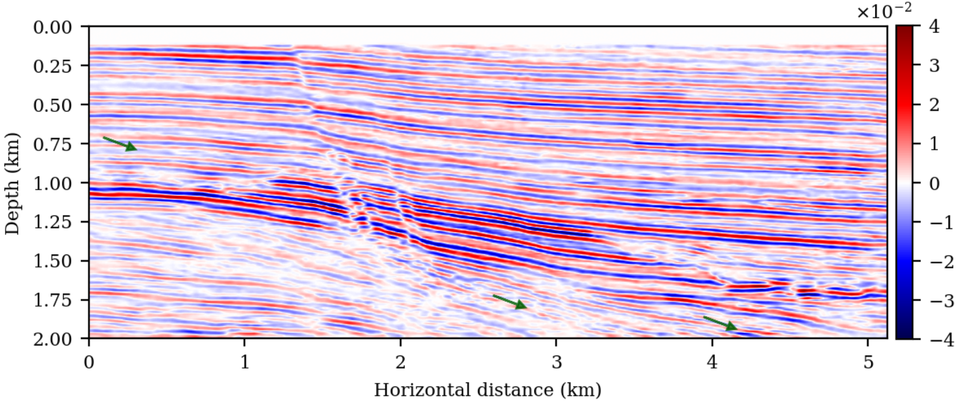

Conditional mean estimate—SNR: 9.66 dB

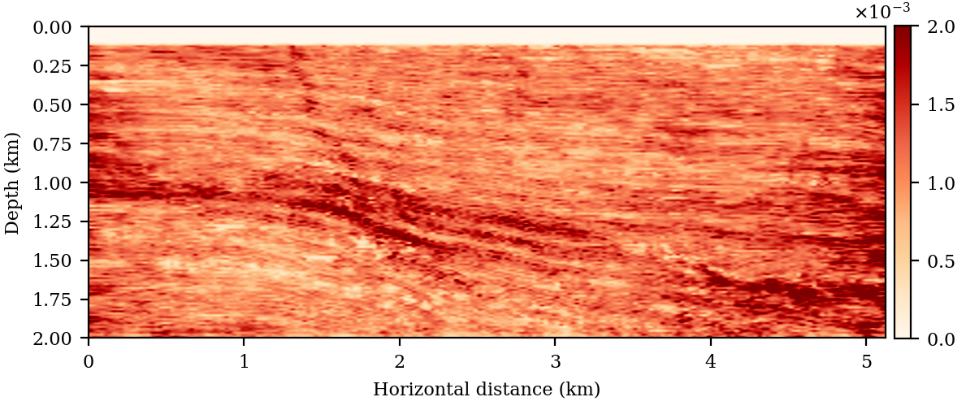
×10−3
2.0
1.5
1.0
0.5
0.0
0.00
0.25
0.50
0.75
1.00
1.25
1.50
1.75
2.00
Depth (km)
0
1
2
3
4
5
Horizontal distance (km)

Imaging UQ

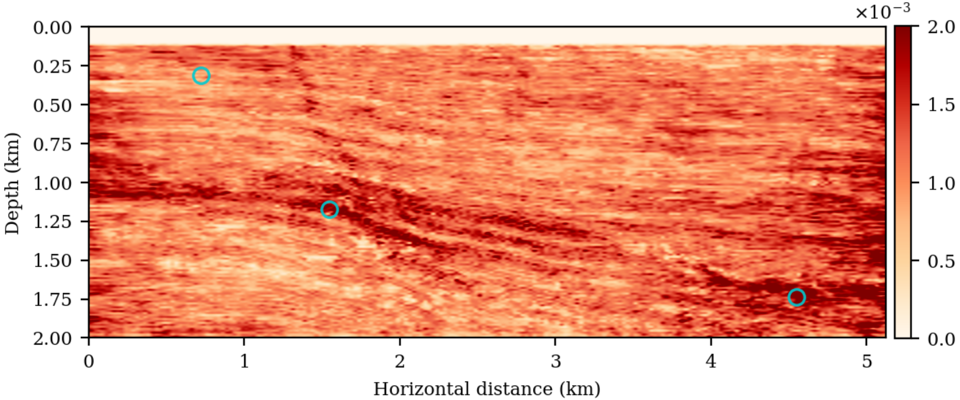
×10^−3
2.0
1.5
1.0
0.5
0.0
0.00
0.25
0.50
0.75
1.00
1.25
1.50
1.75
2.00
Depth (km)
0
1
2
3
4
5
Horizontal distance (km)

Imaging UQ

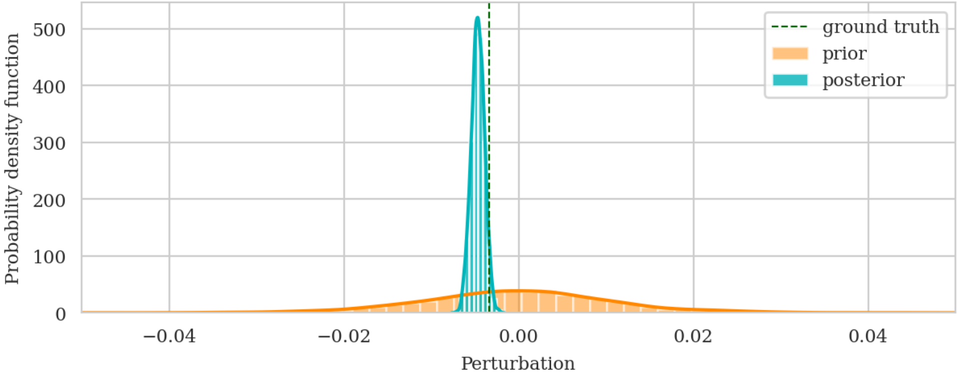

Pointwise marginals at $(0.73\ \mathrm{km},\ 0.32\ \mathrm{km})$

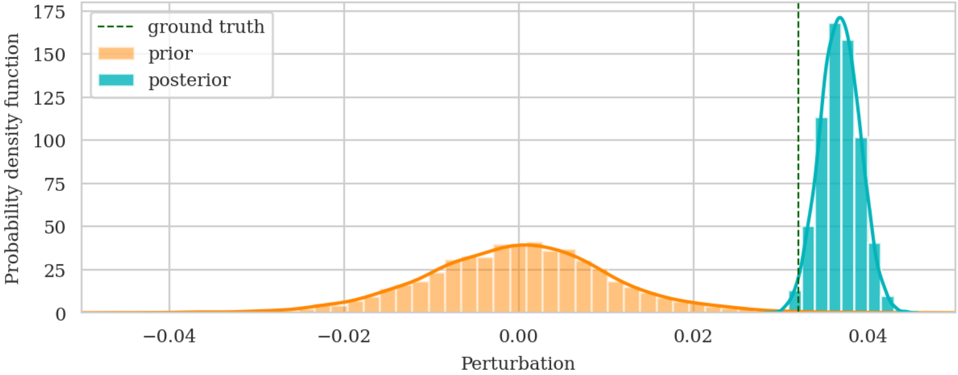

Pointwise marginals at $(1.55\ \mathrm{km},\ 1.18\ \mathrm{km})$

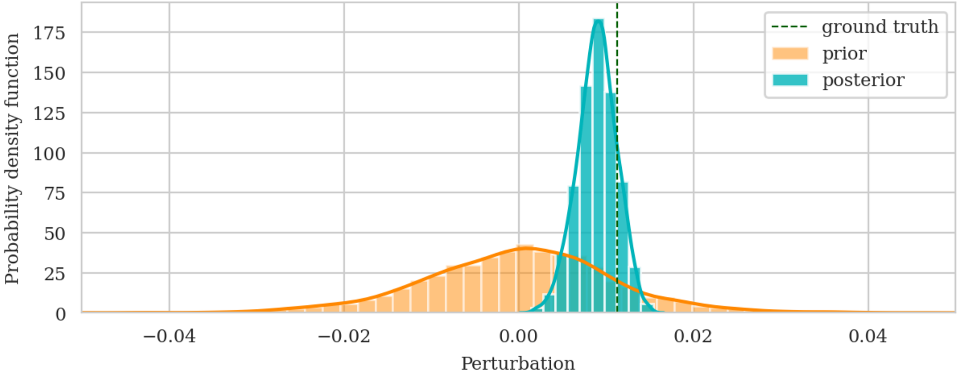

Pointwise marginals at $(4.55\ \mathrm{km},\ 1.74\ \mathrm{km})$

Sampling from the posterior, $\pi_{\mathbf{w}|\delta\mathbf{d}}$

stochastic gradient Langevin dynamics (SGLD)

SGLD—an stochastic-approximation based MCMC sampling approach

$$\mathbf{w}_{k+1} = \mathbf{w}_k + \frac{\epsilon}{2}\mathbf{M}\nabla_{\mathbf{w}}\left[n_s \log \pi_{\text{like}}\left(\delta\mathbf{d}_i \mid \mathbf{w}_k\right) + \log \pi_{\text{prior}}\left(\mathbf{w}_k\right)\right] + \boldsymbol{\eta}_k, \quad \boldsymbol{\eta}_k \sim \mathrm{N}(\mathbf{0}, \epsilon\mathbf{M}),$$

Max Welling and Yee Whye Teh. "Bayesian Learning via Stochastic Gradient Langevin Dynamics". In: *Proceedings of the 28th International Conference on International Conference on Machine Learning*. ICML'11. 2011, pp. 681–688. DOI: 10.5555/3104482.3104568.

Chunyuan Li et al. "Preconditioned Stochastic Gradient Langevin Dynamics for Deep Neural Networks". In: *Proceedings of the Thirtieth AAAI Conference on Artificial Intelligence*. AAAI'16. 2016, pp. 1788–1794. DOI: 10.5555/3016100.3016149.

Devito4PyTorch

integrating Devito's PDE solvers into PyTorch

Ali Siahkoohi, Mathias Louboutin, and Felix Herrmann. *slimgroup/Devito4PyTorch*. 2020. URL: https://github.com/slimgroup/Devito4PyTorch.

Horizon tracking and uncertainty analysis

Contribution

propagate uncertainties from imaging into horizon tracking

i.e., characterizing $\pi_{\mathbf{h}|\delta\mathbf{d}}$*

* $\mathbf{h}$ horizons (random variable)

Assumption

horizon tracker does not directly use observed data

Horizon tracking inference

$$\mathbb{E}_{\mathbf{h}\sim\pi_{\mathbf{h}|\delta\mathbf{d}}}\left[f\left(\mathbf{h}\right)\right] = \underbrace{\mathbb{E}_{\delta\mathbf{m}\sim\pi_{\delta\mathbf{m}|\delta\mathbf{d}}}\underbrace{\mathbb{E}_{\mathbf{h}\sim\pi_{\mathbf{h}|\delta\mathbf{m}}}\left[f\left(\mathbf{h}\right)\right]}_{\text{nonuniqueness in horizon tracking}}}_{\text{nonuniqueness in seismic imaging}}$$

arbitrary function, f—e.g.,

$$f(\mathbf{h}) = \mathbf{h}$$

$$f(\mathbf{h}) = (\mathbf{h} - \mathbb{E}[\mathbf{h}]) \odot (\mathbf{h} - \mathbb{E}[\mathbf{h}])$$

Automatic horizon tracker, $\mathcal{H}$

uses local slopes of the image

needs *control points*

open-source software

Xinming Wu and Sergey Fomel. "Least-squares horizons with local slopes and multi-grid correlations". In: *GEOPHYSICS* 83 (4 2018), pp. IM29–IM40. DOI: 10.1190/geo2017-0830.1. URL: https://doi.org/10.1190/geo2017-0830.1.

Xinming Wu and Sergey Fomel. *xinwucwp/mhe*. 2018. URL: https://github.com/xinwucwp/mhe.

deterministic horizon tracker, $\mathcal{H}$

$$\mathbb{E}_{\mathbf{h}\sim\pi_{\mathbf{h}|\delta\mathbf{d}}}\left[f\left(\mathbf{h}\right)\right]\approx\frac{1}{n_{\mathrm{w}}}\sum_{j=1}^{n_{\mathrm{w}}}f\left(\mathcal{H}(g\left(\mathbf{z},\widehat{\mathbf{w}}_j\right))\right)$$

samples from posterior, $\left\{\widehat{\mathbf{w}}_j\right\}_{j=1}^{n_{\mathrm{w}}}\sim\pi_{\mathbf{w}|\delta\mathbf{d}}(\mathbf{w}\mid\{\delta\mathbf{d}_i\}_{i=1}^{n_s})$

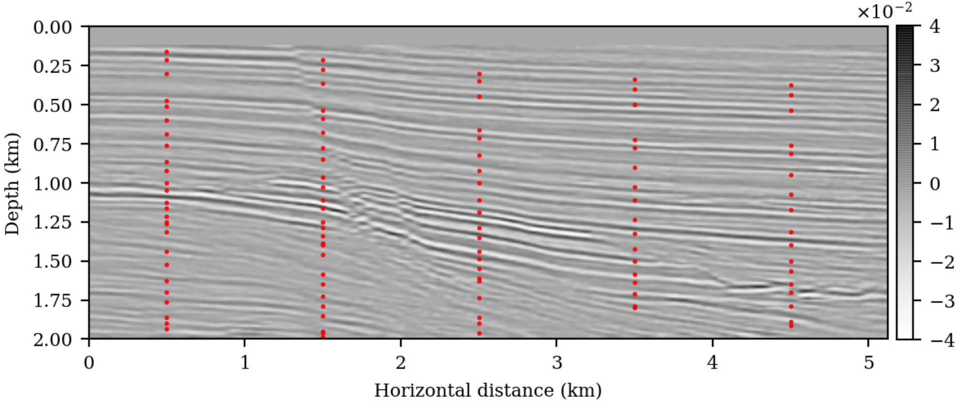

Five sets of control points identifying 25 horizons of interest

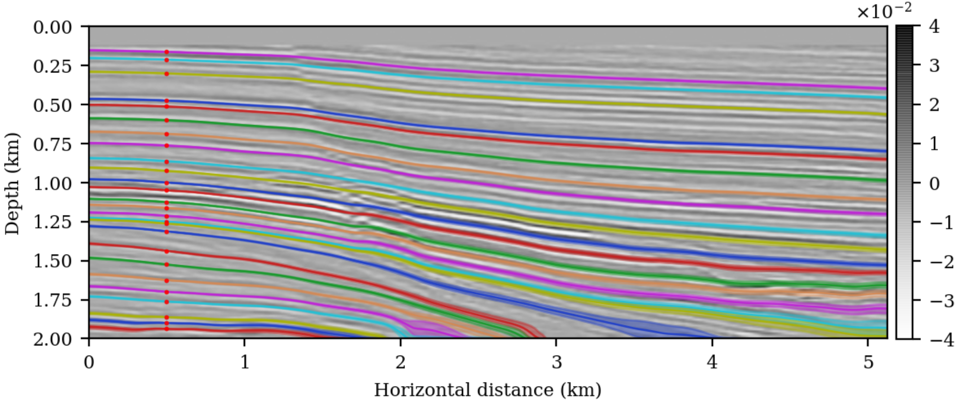

Uncertainty in horizon tracking due to uncertainties in imaging

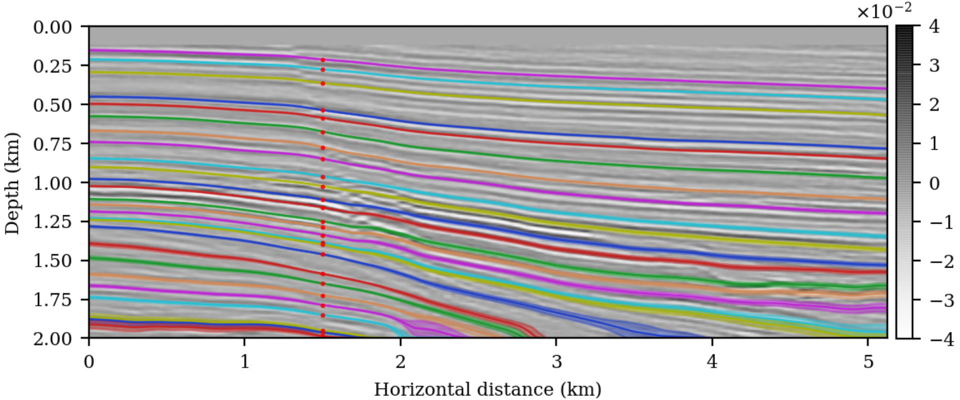

Uncertainty in horizon tracking due to uncertainties in imaging

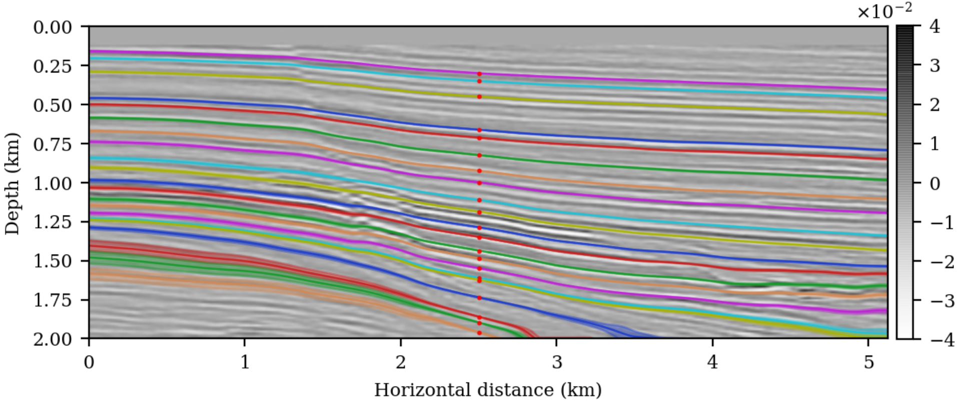

Uncertainty in horizon tracking due to uncertainties in imaging

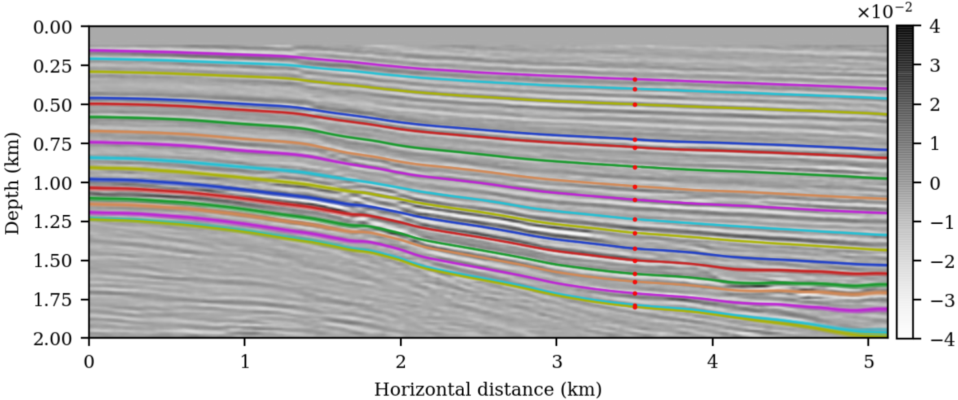

Uncertainty in horizon tracking due to uncertainties in imaging

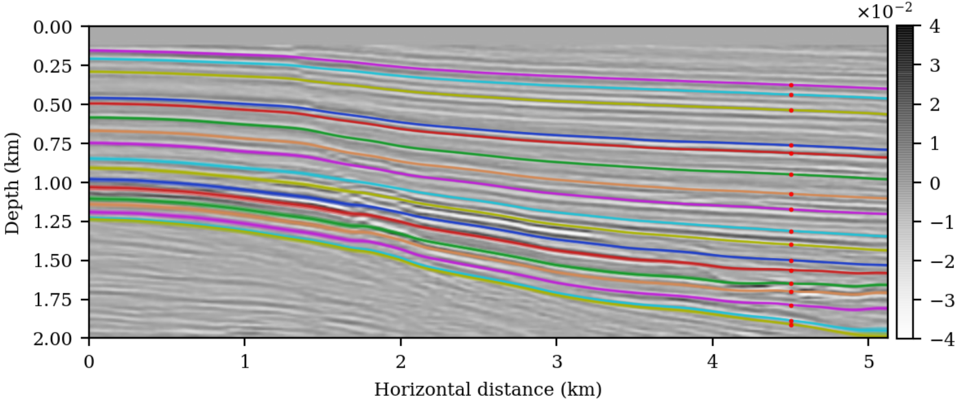

Uncertainty in horizon tracking due to uncertainties in imaging

nondeterministic horizon tracker, $\mathcal{H}$

$$\mathbb{E}_{\mathbf{h}\sim\pi_{\mathbf{h}|\delta\mathbf{d}}}\left[f\left(\mathbf{h}\right)\right] \approx \frac{1}{n_c n_{\mathrm{w}}} \sum_{j=1}^{n_{\mathrm{w}}} \sum_{k=1}^{n_c} f\left(\mathcal{H}(\mathbf{c}_k, g\left(\mathbf{z}, \widehat{\mathbf{w}}_j\right))\right)$$

sets of control points, $\{\mathbf{c}_k\}_{k=1}^{n_c}$

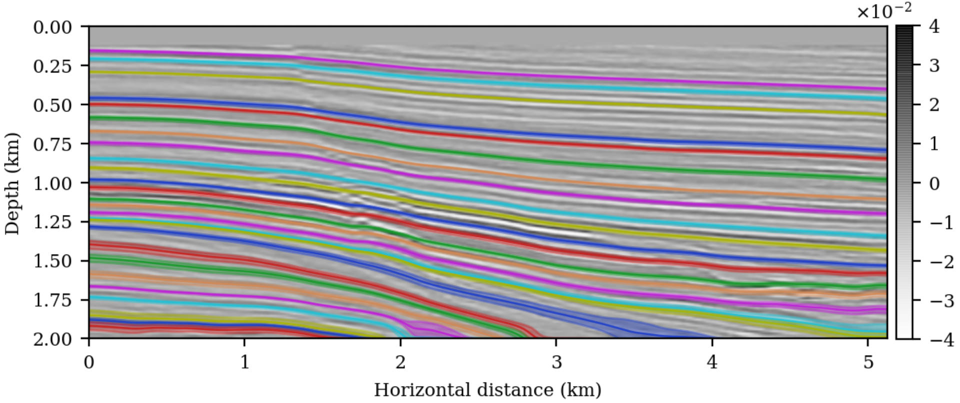

Uncertainty in horizon tracking due uncertainties in imaging and control points

Conclusions

imaging w/ deep prior—expensive but circumvents artifacts

SGLD—reasonable first and second moments of posterior

uncertainties from imaging affect deep, close to boundary, and complex horizons

Contributions

regularization w/ deep priors

imaging uncertainty analysis via SGLD

propagate uncertainties from imaging into horizon tracking

github.com/slimgroup/Software.SEG2020